From spatial symmetry to vibrational spectroscopy of single-walled nanotubes

2003 J. Phys.: Condens. Matter 15 S2489

(http://iopscience.iop.org/0953-8984/15/34/302)

INSTITUTE OF PHYSICS PUBLISHING JOURNAL OF PHYSICS: CONDENSED MATTER

J. Phys.: Condens. Matter **15** (2003) S2489–S2500 PII: S0953-8984(03)64059-2

From spatial symmetry to vibrational spectroscopy of single-walled nanotubes

Ofir E Alon

Theoretische Chemie, Physikalisch-Chemisches Institut, Universität Heidelberg, Im Neuenheimer Feld 229, D-69120 Heidelberg, Germany

E-mail: ofir@tc.pci.uni-heidelberg.de

Received 29 May 2003
Published 15 August 2003
Online at stacks.iop.org/JPhysCM/15/S2489

Abstract

The classification of a molecule's spatial symmetry is an essential initial step in predicting its vibrational spectra. When a (chemical) substitution is made, the relationship between the spatial symmetries of the molecule and its derivatives governs the differences between their corresponding vibrational spectra. These text-book statements of molecular spectroscopy have also found recent and successful applications with much larger molecules, namely single-walled nanotubes. The purpose of this work is to review the profound interplay between the spatial symmetry and the numbers of Raman- and infrared-active vibrations in single-walled carbon and boron nitride nanotubes.

1. Introduction

Since their discovery by Iijima at the beginning of the 1990s [1], carbon nanotubes (CNTs) have attracted enormous attention from both experimentalists and theoreticians for their novel properties and potential applications (see, for example, [2, 3] and references therein). A CNT is a synthesized allotropic form of carbon (see, for example, [4] for a review of their physical properties). Single-walled CNTs (hereafter called CNTs), to which we will restrict our attention, can be viewed as cylinders made of graphite sheets (graphene). The infinite-order, two-dimensional (2D) translational symmetries of the hexagonal net (for which the plane group is $p6mm$) can transform into various finite-order symmetries once the graphene plane is transformed (rolled) into a CNT cylinder. The order and character of the resulting symmetries depend on the way the graphene boundaries are connected to each other to form the cylinder.

Figure 1 illustrates the classification according to the pair of indices (n, m), representing different CNTs. The (n, m) CNT is formed by rolling the graphene sheet along the chiral vector

$$\boldsymbol{C}_{\mathrm{h}} = n\boldsymbol{a}_1 + m\boldsymbol{a}_2 \tag{1}$$

(where $\boldsymbol{a}_1$ and $\boldsymbol{a}_2$ are the two primitive vectors of the honeycomb lattice), such that its origin O and its end-point O' coincide on the CNT. If the graphene sheet is rolled along the $n\boldsymbol{a}_1$ direction, then an achiral zigzag CNT—classified by the pair of indices $(n, 0)$—is formed.

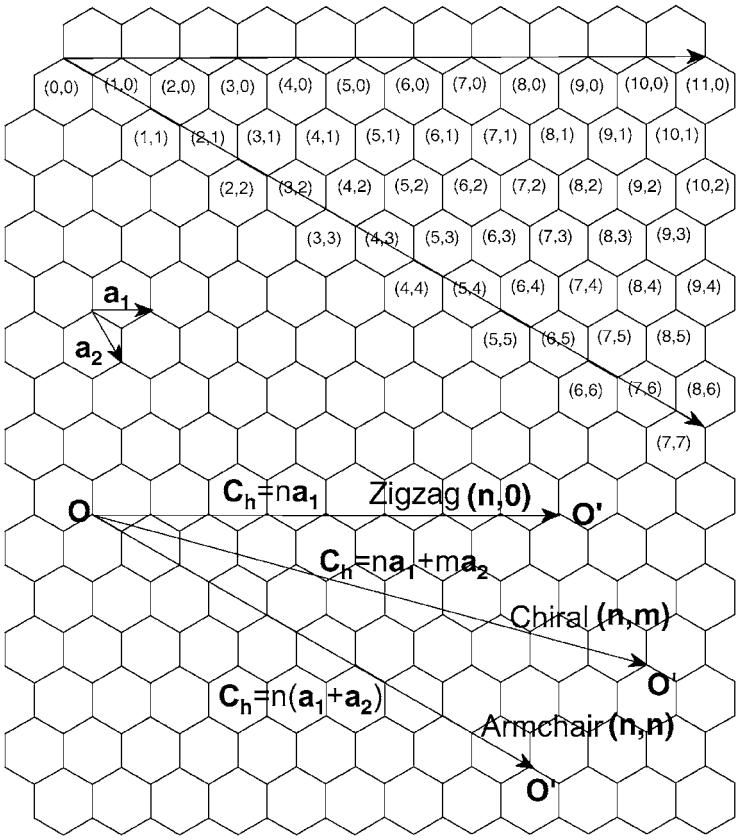

Figure 1. The classification of CNTs according to the pair of indices (n, m). $\boldsymbol{a}_1$ and $\boldsymbol{a}_2$ are the two primitive vectors of the honeycomb lattice. The chiral vectors $\boldsymbol{C}_\mathrm{h} = \boldsymbol{OO'}$ are shown for zigzag, chiral and armchair CNTs.

If the graphene sheet is rolled along the $n(\boldsymbol{a}_1 + \boldsymbol{a}_2)$ direction, then an achiral armchair CNT—classified by the pair of indices (n, n)—is formed. In all other cases, i.e. whenever $0 < m < n$, a chiral CNT is formed.

The primitive translation vector of the CNT *unit cell*, $\boldsymbol{T}_z$, is given by

$$\boldsymbol{T}_z = \frac{1}{d_\mathrm{R}}[(2m+n)\boldsymbol{a}_1 - (2n+m)\boldsymbol{a}_2], \tag{2}$$

where d_R is the greatest common divisor of $2n + m$ and $2m + n$ [4]. From the size of the unit cell, which is defined by the orthogonal vectors $\boldsymbol{T}_z$ and $\boldsymbol{C}_\mathrm{h}$, we can readily find the number of hexagons per unit cell:

$$N = \frac{2(m^2 + mn + n^2)}{d_\mathrm{R}}. \tag{3}$$

Note that each hexagon contains two carbon atoms.

A boron nitride nanotube (BNT) is a recently synthesized [5, 6] novel type of material that combines stable insulating properties [7, 8] and high strength [9]. Owing to the subset relation between the plane groups of 2D hexagonal boron nitride and graphite nets,

$$p3m1 \subseteq p6mm, \tag{4}$$

single-walled BNTs (hereafter called BNTs) are characterized, as for CNTs, by the pair of indices n and m: i.e. armchair $(n, m = n)$; zigzag $(n, m = 0)$; and chiral $(n, 0 < m < n)$. Thus, the (n, m) BNT and CNT possess the same lattice period $\boldsymbol{T}_z$ and number N of hexagons within their unit cells. *Ab initio* studies of the spatial *structure* of BNTs have predicted the buckling of B–N bonds, i.e. the formation of a concentric inner 'B-cylinder' and outer 'N-cylinder' [8, 10].

2. Active phonons in single-walled carbon nanotubes

The classification of CNT symmetries is an essential stage in predicting their physical properties, among which are active infrared (IR) and Raman vibrations (see, for example, [4] and references therein).

In early CNT research, the determination of optically active phonon modes in achiral CNTs was performed with symmorphic rod groups (see [4] and references therein). To account for the inversion symmetry operation, unit cells possessing the point groups $\mathcal{D}_{nh}$ or $\mathcal{D}_{nd}$ for even or odd ns, respectively, were chosen for the $(n, 0)$ zigzag and (n, n) armchair CNTs. This led to the prediction of 15–16 Raman-active phonon modes for infinitely long armchair CNTs [4], with frequencies of up to about 1600 cm^{-1} (see [11] for a recent calculation of the frequencies of vibrationally active modes in achiral CNTs). On the basis of calculations of Raman line intensities, however, only seven of the above-predicted modes were found to be intense (in the low- and high-frequency zones). The rest (in the intermediate-frequency zone) were found to have no intensity for infinite nanotubes [12], but some intensity for finite nanotubes [13]. These latter predictions, based on Raman line intensities, have found clear fingerprints in Raman scattering experiments from CNT ropes (see, for example, [14, 15]).

Following Damnjanović *et al* [16, 17], one learned in 1999 that achiral CNTs also possess a screw axis of the order of $2n$ and n glide planes. Due to these operations, the symmetry of achiral CNTs is described by non-symmorphic rod groups. This higher symmetry has been shown to have a dramatic effect on the vibrational spectra of achiral CNTs [18]. In particular, armchair CNTs have been shown to possess only eight Raman-active vibrations, which corroborated the experimental data (see, for example, [14, 15]).

The determination of the numbers of Raman- and IR-active vibrations in chiral CNTs in the 'early' days of CNT studies was performed with commutative non-symmorphic rod groups (see [4] and references therein). The point group of the rod group of the (n, m) chiral CNT was taken to be $\mathcal{C}_N$, where N is given by equation (3). In 1999, Damnjanović *et al* [16, 17] showed that chiral CNTs also possess perpendicular C_2 axes. The existence of these previously 'overlooked' symmetry operations constituted geometrical proof that chiral CNTs possess the spatial symmetry of non-commutative non-symmorphic rod groups [16, 17]. In turn, this higher symmetry led to the conclusion of there being fewer active vibrations [18].

2.1. Achiral carbon nanotubes

Consider the achiral CNTs that possess the rotation axis of order n, i.e. the $(n, 0)$ zigzag or (n, n) armchair CNTs. The non-symmorphic rod group [16, 17] describing the achiral CNTs with index n can be decomposed in the following manner (the 13th family of rod groups [19]):

$$\begin{aligned}\mathcal{G}[n] &= \mathcal{L}_{T_z} \times \mathcal{D}_{n\mathrm{h}} \times [\boldsymbol{E} \oplus \boldsymbol{S}_{2n}] = \mathcal{L}_{T_z} \times \mathcal{D}_{n\mathrm{d}} \times [\boldsymbol{E} \oplus \boldsymbol{S}_{2n}] \\ &= \mathcal{L}_{T_z} \times [\mathcal{D}_{n\mathrm{h}}|_{z=0} \oplus (\mathcal{D}_{n\mathrm{d}}|_{z=T_z/4} \ominus \mathcal{C}_{n\mathrm{v}}) \oplus \mathcal{C}_{n\mathrm{v}} \times \boldsymbol{S}_{2n}], \end{aligned} \tag{5}$$

where the reference point $z = 0$ denotes the crossing of horizontal, $\boldsymbol{\sigma}_\mathrm{h}$, and vertical, $\boldsymbol{\sigma}_\mathrm{v}$, reflection planes (see figure 2), $\mathcal{L}_{T_z}$ is the 1D translation group with the primitive translation

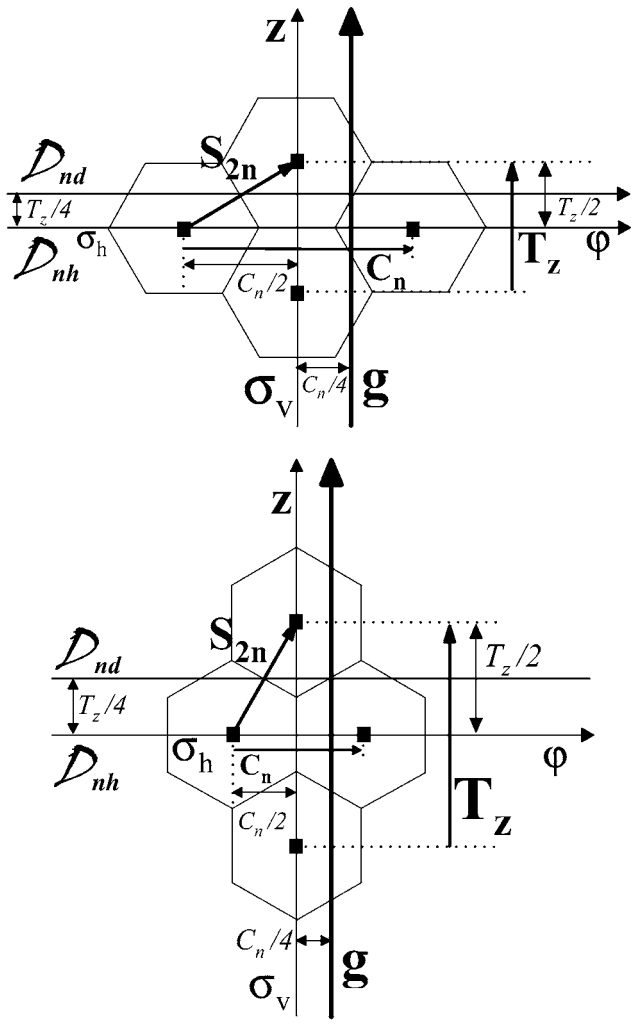

Figure 2. The 2D projection of various symmetries in achiral CNTs (armchair segment—top; zigzag segment—bottom): $\boldsymbol{T}_z$ is the primitive translation; $\boldsymbol{S}_{2n}$ is the screw axis with non-primitive translation and rotation, denoted by $T_z/2$ and $C_n/2$, respectively; $\boldsymbol{g}$ is a glide plane; $\mathcal{D}_{nh}|_{z=0}$ and $\mathcal{D}_{nd}|_{z=T_z/4}$ are the corresponding point-group operations, among which $\boldsymbol{\sigma}_h$, $\boldsymbol{\sigma}_v$ and $\boldsymbol{C}_n$ are denoted. Note the $T_z/4$ shift between $\mathcal{D}_{nh}|_{z=0}$ and $\mathcal{D}_{nd}|_{z=T_z/4}$, which coexist in all achiral CNTs.

$T_z = |\boldsymbol{T}_z|$ and $\boldsymbol{E}$ is the identity operation. The screw axis $\boldsymbol{S}_{2n} = (z \to z + \frac{T_z}{2}, \varphi \to \varphi + \frac{\pi}{n})$ involves the lattice's smallest non-primitive translation and rotation. The subtraction of the point group $\mathcal{C}_{nv}$ in equation (5) reflects the set relation $\mathcal{D}_{nh}|_{z=0} \cap \mathcal{D}_{nd}|_{z=T_z/4} = \mathcal{C}_{nv}$, which is valid for all n. The glide plane $\boldsymbol{g}$ is also presented in figure 2. It fulfils the multiplicative relation $\boldsymbol{g} = \boldsymbol{S}_{2n}\boldsymbol{\sigma}_v$. The existence of n distinct glide planes in $\mathcal{G}[n]$ stems from the last term in equation (5).

The point group of the rod group, $\mathcal{G}_0[n]$, is obtained by setting all translations (including the non-primitive ones) in $\mathcal{G}[n]$ equal to zero. From equation (5), we obtain

$$\mathcal{G}_0[n] = \mathcal{D}_{nh} \times [\boldsymbol{E} \oplus C_{2n}] = \mathcal{D}_{nd} \times [\boldsymbol{E} \oplus C_{2n}] = \mathcal{D}_{2nh}, \tag{6}$$

where $C_{2n} = (\varphi \to \varphi + \frac{\pi}{n})$ is the rotation embedded in $\boldsymbol{S}_{2n}$.

Aiming at characterizing the symmetries of phonons at the $\Gamma(k = 0)$-point, we would like to discuss the irreducible representations (irreps) of $\mathcal{G}[n]$ at Γ. As known from the theory of space groups [20], these irreps are in a one-to-one correspondence with the irreps of $\mathcal{G}_0[n] = \mathcal{D}_{2n\mathrm{h}}$. Recall that the character table of $\mathcal{D}_{2n\mathrm{h}}$ possesses $2n + 6$ irreps [21]:

$$\Gamma_{\mathcal{D}_{2n\mathrm{h}}} = \mathrm{A_{1g}} \oplus \mathrm{A_{2g}} \oplus \mathrm{B_{1g}} \oplus \mathrm{B_{2g}} \oplus \mathrm{A_{1u}} \oplus \mathrm{A_{2u}} \oplus \mathrm{B_{1u}} \oplus \mathrm{B_{2u}} \oplus \bigoplus_{j=1}^{n-1} \{\mathrm{E}_{j\mathrm{g}} \oplus \mathrm{E}_{j\mathrm{u}}\}. \tag{7}$$

Next, we would like to determine the symmetries of the $6N$ phonon modes at the Γ-point and how many modes are Raman or IR active. Recall that, for achiral CNTs, $N = 2n$. At this point we have to differentiate between $(n, 0)$ zigzag and (n, n) armchair CNTs, due to the differences in the arrangements of atoms inside their unit cells. The $6N$ phonon modes transform according to the following irreps for zigzag CNTs:

$$\begin{aligned}
\Gamma_{6N}^{\mathrm{zig},n\in\mathrm{evens}} &= \Gamma_{\mathrm{a}}^{\mathrm{zig},n\in\mathrm{evens}} \otimes \Gamma_{\mathrm{v}} = 2\mathrm{A_{1g}} \oplus \mathrm{A_{2g}} \oplus 2\mathrm{B_{1g}} \oplus \mathrm{B_{2g}} \oplus \mathrm{A_{1u}} \\
&\quad \oplus 2\mathrm{A_{2u}} \oplus \mathrm{B_{1u}} \oplus 2\mathrm{B_{2u}} \oplus \bigoplus_{j=1}^{n-1} \{3\mathrm{E}_{j\mathrm{g}} \oplus 3\mathrm{E}_{j\mathrm{u}}\}, \\
\Gamma_{6N}^{\mathrm{zig},n\in\mathrm{odds}} &= \Gamma_{\mathrm{a}}^{\mathrm{zig},n\in\mathrm{odds}} \otimes \Gamma_{\mathrm{v}} = 2\mathrm{A_{1g}} \oplus \mathrm{A_{2g}} \oplus \mathrm{B_{1g}} \oplus 2\mathrm{B_{2g}} \oplus \mathrm{A_{1u}} \\
&\quad \oplus 2\mathrm{A_{2u}} \oplus 2\mathrm{B_{1u}} \oplus \mathrm{B_{2u}} \oplus \bigoplus_{j=1}^{n-1} \{3\mathrm{E}_{j\mathrm{g}} \oplus 3\mathrm{E}_{j\mathrm{u}}\},
\end{aligned} \tag{8}$$

where

$$\begin{aligned}
\Gamma_{\mathrm{a}}^{\mathrm{zig},n\in\mathrm{evens}} &= \mathrm{A_{1g}} \oplus \mathrm{B_{1g}} \oplus \mathrm{A_{2u}} \oplus \mathrm{B_{2u}} \oplus \bigoplus_{j=1}^{n-1} \{\mathrm{E}_{j\mathrm{g}} \oplus \mathrm{E}_{j\mathrm{u}}\}, \\
\Gamma_{\mathrm{a}}^{\mathrm{zig},n\in\mathrm{odds}} &= \mathrm{A_{1g}} \oplus \mathrm{B_{2g}} \oplus \mathrm{A_{2u}} \oplus \mathrm{B_{1u}} \oplus \bigoplus_{j=1}^{n-1} \{\mathrm{E}_{j\mathrm{g}} \oplus \mathrm{E}_{j\mathrm{u}}\},
\end{aligned} \tag{9}$$

stand for the reducible representations of the carbon atoms' positions inside the unit cells and $\Gamma_{\mathrm{v}} = \mathrm{A_{2u}} \oplus \mathrm{E_{1u}}$ is the vector representation. Similarly, the $6N$ phonon modes for armchair CNTs transform according to the following irreps:

$$\begin{aligned}
\Gamma_{6N}^{\mathrm{arm},n\in\mathrm{evens}} &= \Gamma_{\mathrm{a}}^{\mathrm{arm},n\in\mathrm{evens}} \otimes \Gamma_{\mathrm{v}} = 2\mathrm{A_{1g}} \oplus 2\mathrm{A_{2g}} \oplus 2\mathrm{B_{1g}} \oplus 2\mathrm{B_{2g}} \oplus \mathrm{A_{1u}} \oplus \mathrm{A_{2u}} \oplus \mathrm{B_{1u}} \oplus \mathrm{B_{2u}} \\
&\quad \oplus 2\mathrm{E_{1g}} \oplus 4\mathrm{E_{2g}} \oplus 2\mathrm{E_{3g}} \oplus 4\mathrm{E_{4g}} \oplus \cdots \oplus (3 + (-1)^{n-1})\mathrm{E}_{(n-1)\mathrm{g}} \\
&\quad \oplus 4\mathrm{E_{1u}} \oplus 2\mathrm{E_{2u}} \oplus 4\mathrm{E_{3u}} \oplus 2\mathrm{E_{4u}} \oplus \cdots \oplus (3 - (-1)^{n-1})\mathrm{E}_{(n-1)\mathrm{u}}, \\
\Gamma_{6N}^{\mathrm{arm},n\in\mathrm{odds}} &= \Gamma_{\mathrm{a}}^{\mathrm{arm},n\in\mathrm{odds}} \otimes \Gamma_{\mathrm{v}} = 2\mathrm{A_{1g}} \oplus 2\mathrm{A_{2g}} \oplus \mathrm{B_{1g}} \oplus \mathrm{B_{2g}} \oplus \mathrm{A_{1u}} \oplus \mathrm{A_{2u}} \oplus 2\mathrm{B_{1u}} \oplus 2\mathrm{B_{2u}} \\
&\quad \oplus 2\mathrm{E_{1g}} \oplus 4\mathrm{E_{2g}} \oplus 2\mathrm{E_{3g}} \oplus 4\mathrm{E_{4g}} \oplus \cdots \oplus (3 + (-1)^{n-1})\mathrm{E}_{(n-1)\mathrm{g}} \\
&\quad \oplus 4\mathrm{E_{1u}} \oplus 2\mathrm{E_{2u}} \oplus 4\mathrm{E_{3u}} \oplus 2\mathrm{E_{4u}} \oplus \cdots \oplus (3 - (-1)^{n-1})\mathrm{E}_{(n-1)\mathrm{u}},
\end{aligned} \tag{10}$$

where

$$\begin{aligned}
\Gamma_{\mathrm{a}}^{\mathrm{arm},n\in\mathrm{evens}} &= \mathrm{A_{1g}} \oplus \mathrm{A_{2g}} \oplus \mathrm{B_{1g}} \oplus \mathrm{B_{2g}} \oplus 2\bigoplus_{j=2l}^{n-1} \mathrm{E}_{j\mathrm{g}} \oplus 2\bigoplus_{j=2l-1}^{n-1} \mathrm{E}_{j\mathrm{u}}, \\
\Gamma_{\mathrm{a}}^{\mathrm{arm},n\in\mathrm{odds}} &= \mathrm{A_{1g}} \oplus \mathrm{A_{2g}} \oplus \mathrm{B_{1u}} \oplus \mathrm{B_{2u}} \oplus 2\bigoplus_{j=2l}^{n-1} \mathrm{E}_{j\mathrm{g}} \oplus 2\bigoplus_{j=2l-1}^{n-1} \mathrm{E}_{j\mathrm{u}},
\end{aligned} \tag{11}$$

stand for the reducible representations of the carbon atoms' positions inside the unit cells. Of these modes, those that transform according to $\Gamma_{\mathrm{t}} = \mathrm{A_{1g}} \oplus \mathrm{E_{1g}} \oplus \mathrm{E_{2g}}$ (the tensor

representation) or $\Gamma_{\rm v}$ are Raman or IR active, respectively. Out of the $6N$ phonon modes, four (which transform as $\Gamma_{\rm v}$ and $\Gamma_{R_z} = {\rm A}_{2{\rm g}}$) have vanishing frequencies [4, 22]. Consequently, the symmetries and numbers of optically active phonon modes in zigzag CNTs (with either odd or even index n) are given by [18]:

$$\Gamma^{\rm zig}_{\rm Raman} = 2{\rm A}_{1{\rm g}} \oplus 3{\rm E}_{1{\rm g}} \oplus 3{\rm E}_{2{\rm g}} \Longrightarrow n^{\rm zig}_{\rm Raman} = 8, \tag{12}$$

$$\Gamma^{\rm zig}_{\rm IR} = {\rm A}_{2{\rm u}} \oplus 2{\rm E}_{1{\rm u}} \Longrightarrow n^{\rm zig}_{\rm IR} = 3, \tag{13}$$

and, in armchair CNTs (with either odd or even index n) [18], by:

$$\Gamma^{\rm arm}_{\rm Raman} = 2{\rm A}_{1{\rm g}} \oplus 2{\rm E}_{1{\rm g}} \oplus 4{\rm E}_{2{\rm g}} \Longrightarrow n^{\rm arm}_{\rm Raman} = 8, \tag{14}$$

$$\Gamma^{\rm arm}_{\rm IR} = 3{\rm E}_{1{\rm u}} \Longrightarrow n^{\rm arm}_{\rm IR} = 3. \tag{15}$$

Thus, the numbers of Raman- and IR-active phonon modes were found to be fixed for all zigzag and armchair CNTs [18], as had previously been predicted by Dresselhaus and co-workers using the *subgroup* point groups $\mathcal{D}_{n{\rm h}}, \mathcal{D}_{n{\rm d}} \subseteq \mathcal{D}_{2n{\rm h}}$ (see [4] and references therein). Due to the higher rod group and factor group symmetries [16, 17] there are much fewer active modes: eight (Raman) and three (IR) [18], instead of 15–16 and 7–8 [4], respectively.

2.2. Chiral carbon nanotubes

To discuss the numbers of Raman- and IR-active vibrations in chiral CNTs, we start with their spatial symmetry. The non-symmorphic rod group that describes the (n, m) chiral CNT [16, 17] can be decomposed as follows (the 5th family of rod groups [19]):

$$\mathcal{G}[N] = \mathcal{L}_{T_z} \times \mathcal{D}_d \times \left[\sum_{j=0}^{\frac{N}{d}-1} \!\!\!\!\!\!\bigcirc\;\; \boldsymbol{S}^j_{N/d}\right] = \mathcal{L}_{T_z} \times \mathcal{D}_1 \times \left[\sum_{j=0}^{N-1} \!\!\!\!\!\!\bigcirc\;\; \boldsymbol{S}^j_{N}\right], \tag{16}$$

where d is the greatest common divisor of n and m, and $\boldsymbol{S}_{N/d}$ and $\boldsymbol{S}_N$ are screw-axis operations with the orders of N/d and N, respectively. The point group of the rod group is readily obtained from equation (16):

$$\mathcal{G}_0[N] = \sum_{j=0}^{\frac{N}{d}-1} \!\!\!\!\!\!\bigcirc\;\; C^j_{N/d} \times \mathcal{D}_d = \sum_{j=0}^{N-1} \!\!\!\!\!\!\bigcirc\;\; C^j_N \times \mathcal{D}_1 = \mathcal{D}_N, \tag{17}$$

where $C_{N/d} = (\varphi \to \varphi + \frac{2d\pi}{N})$ and $C_N = (\varphi \to \varphi + \frac{2\pi}{N})$ are the rotations embedded in $\boldsymbol{S}^j_{N/d}$ and $\boldsymbol{S}_N$, respectively. As mentioned above, this higher symmetry ($\mathcal{D}_N \supseteq \mathcal{C}_N$) led to the reduction of the numbers of optically active phonon modes in chiral CNTs [18].

Analogously to the treatment given above for achiral CNTs, we would like to discuss the irreps of $\mathcal{G}_0[N]$ $\mathcal{D}_N$ for chiral CNTs. Recall that the character table of $\mathcal{D}_N$ possesses $\frac{N}{2} + 3$ irreps (N is always even for CNTs) [21]:

$$\Gamma_{\mathcal{D}_N} = {\rm A}_1 \oplus {\rm A}_2 \oplus {\rm B}_1 \oplus {\rm B}_2 \oplus \sum_{j=1}^{\frac{N}{2}-1} \!\!\!\!\!\!\bigcirc\;\; {\rm E}_j. \tag{18}$$

The $6N$ phonon modes transform according to the following irreps:

$$\Gamma^{\rm ch}_{6N} = \Gamma^{\rm ch}_{\rm a} \otimes \Gamma_{\rm v} = 3{\rm A}_1 \oplus 3{\rm A}_2 \oplus 3{\rm B}_1 \oplus 3{\rm B}_2 \oplus \sum_{j=1}^{\frac{N}{2}-1} \!\!\!\!\!\!\bigcirc\;\; 6{\rm E}_j, \tag{19}$$

where

$$\Gamma^{\rm ch}_{\rm a} = {\rm A}_1 \oplus {\rm A}_2 \oplus {\rm B}_1 \oplus {\rm B}_2 \oplus \sum_{j=1}^{\frac{N}{2}-1} \!\!\!\!\!\!\bigcirc\;\; 2{\rm E}_j, \tag{20}$$

stands for the reducible representation of the carbon atoms' positions inside the unit cell, and $\Gamma_{\mathrm{v}} = \mathrm{A}_2 \oplus \mathrm{E}_1$ is the vector representation. Of these modes, those that transform according to $\Gamma_{\mathrm{t}} = \mathrm{A}_1 \oplus \mathrm{E}_1 \oplus \mathrm{E}_2$ and/or Γ_{v} are Raman and/or IR active, respectively. Four of the $6N$ phonon modes (those which transform as Γ_{v} and $\Gamma_{R_z} = \mathrm{A}_2$) have vanishing frequencies [4, 22]. Consequently, the symmetries and numbers of optically active phonon modes are given by [18]:

$$\Gamma^{\mathrm{ch}}_{\mathrm{Raman}} = 3\mathrm{A}_1 \oplus 5\mathrm{E}_1 \oplus 6\mathrm{E}_2 \Longrightarrow n^{\mathrm{ch}}_{\mathrm{Raman}} = 14, \tag{21}$$

$$\Gamma^{\mathrm{ch}}_{\mathrm{IR}} = \mathrm{A}_2 \oplus 5\mathrm{E}_1 \Longrightarrow n^{\mathrm{ch}}_{\mathrm{IR}} = 6. \tag{22}$$

Thus, the numbers of Raman- and IR-active phonon modes have been found to be independent of the chiral CNT indices (n, m), as had previously been predicted by Dresselhaus and co-workers (see [4] and references therein) using the *subgroup* factor-group $\mathcal{C}_N \subseteq \mathcal{D}_N$. However, due to the higher rod-group and factor-group symmetries, fewer modes were found to be active: 14 (Raman) and six (IR) [18] instead of 15 and nine [4], respectively.

3. Active phonons in single-walled boron nitride nanotubes

The classification of BNT spatial symmetries has been carried out only recently [23, 24]. The profound implications of the symmetry properties of BNTs on physical effects can be seen in, for example, the work of Král *et al* [25], who predicted non-centrosymmetry- and polarity-based photogalvanic effects in BNTs. More specifically, the direction of the induced photocurrent was shown to depend on the BNT chirality. However, *all* armchair BNTs are *centrosymmetric*. Nevertheless, and in contrast to 2D and 3D centrosymmetric and polar crystalline materials, they (should) exhibit the azimuthal photocurrents predicted in [25]. Below we review the determination of the numbers of Raman- and IR-active vibrations in BNTs as well as their *correlation* with those of the corresponding CNTs [24]. Very recently, measurements of IR and Raman spectra of BNTs have been performed for the first time [26], generally corroborating the theoretical predictions. Simultaneously, the frequencies of the active vibrations in BNTs have been calculated [26–29].

3.1. Armchair and zigzag boron nitride nanotubes

Consider the achiral BNTs possessing a rotation axis of order n, i.e. the (n, n) armchair (figure 3) and $(n, 0)$ zigzag (figure 4) BNTs. Unlike the situation for CNTs, these do not possess the same symmetry operations [23, 24], owing to the lower symmetry described in equation (4). Nevertheless, they still possess symmetries of non-symmorphic rod groups because the screw axis $\boldsymbol{S}_{2n}$ 'survives' this symmetry lowering (see figures 3 and 4). More specifically, the (n, n) armchair BNT possesses *horizontal* reflection planes (see figure 3). The lack of C_2 axes (recall that there are no C_2 axes in $p3m1$) leads to the absence of vertical reflection planes in this case. Consequently, the $\mathcal{D}_{n\mathrm{h}}$ and $\mathcal{D}_{n\mathrm{d}}$ point groups in armchair CNTs (see figure 2 (top) and equation (5)) reduce to $\mathcal{C}_{n\mathrm{h}}$ and $\mathcal{S}_{2n}$, respectively (see figure 3). The converse is true for the $(n, 0)$ zigzag BNT, which has *vertical* reflection planes (see figure 4) but no horizontal reflection planes. Consequently, both the $\mathcal{D}_{n\mathrm{h}}$ and $\mathcal{D}_{n\mathrm{d}}$ point groups in zigzag CNTs (see figure 2 (bottom) and equation (5)) reduce to $\mathcal{C}_{n\mathrm{v}}$ (see figure 4). Therefore, the non-symmorphic rod group that describes the (n, n) armchair BNT with (either odd or even) index n [23, 24] can be decomposed in the following manner (the 4th family of rod groups [19]):

$$\begin{aligned}\mathcal{G}^{\mathrm{arm}}[n] &= \mathcal{L}_{T_z} \times \mathcal{C}_{n\mathrm{h}} \times [\boldsymbol{E} \oplus \boldsymbol{S}_{2n}] = \mathcal{L}_{T_z} \times \mathcal{S}_{2n} \times [\boldsymbol{E} \oplus \boldsymbol{S}_{2n}] \\ &= \mathcal{L}_{T_z} \times [\mathcal{C}_{n\mathrm{h}}|_{z=0} \oplus (\mathcal{S}_{2n}|_{z=T_z/4} \ominus \mathcal{C}_n) \oplus \mathcal{C}_n \times \boldsymbol{S}_{2n}].\end{aligned} \tag{23}$$

The reference point $z = 0$ denotes the crossing of horizontal reflection plane, $\boldsymbol{\sigma}_{\mathrm{h}}$, and the n-fold rotation axis, $\boldsymbol{C}_n$ (see figure 3). The subtraction of the point group $\mathcal{C}_n$ in equation (23) reflects

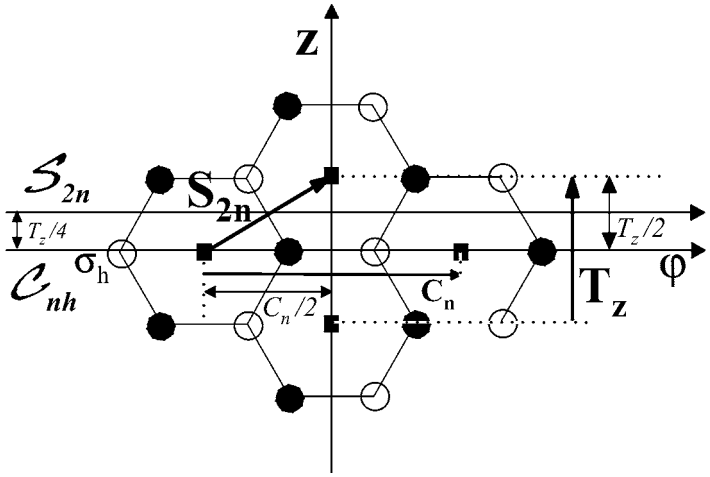

Figure 3. 2D projection of various symmetries in armchair BNTs (●, B; ○, N): $\boldsymbol{T}_z$ is the primitive translation; $\boldsymbol{S}_{2n}$ is the screw axis with non-primitive translation and rotation, denoted by $T_z/2$ and $C_n/2$, respectively; $\mathcal{C}_{n\mathrm{h}}|_{z=0}$ and $\mathcal{S}_{2n}|_{z=T_z/4}$ stand for the corresponding point-group operations, among which $\boldsymbol{\sigma}_\mathrm{h}$ and $\boldsymbol{C}_n$ are denoted. Note the $T_z/4$ shift between $\mathcal{C}_{n\mathrm{h}}|_{z=0}$ and $\mathcal{S}_{2n}|_{z=T_z/4}$, which coexist in all armchair BNTs.

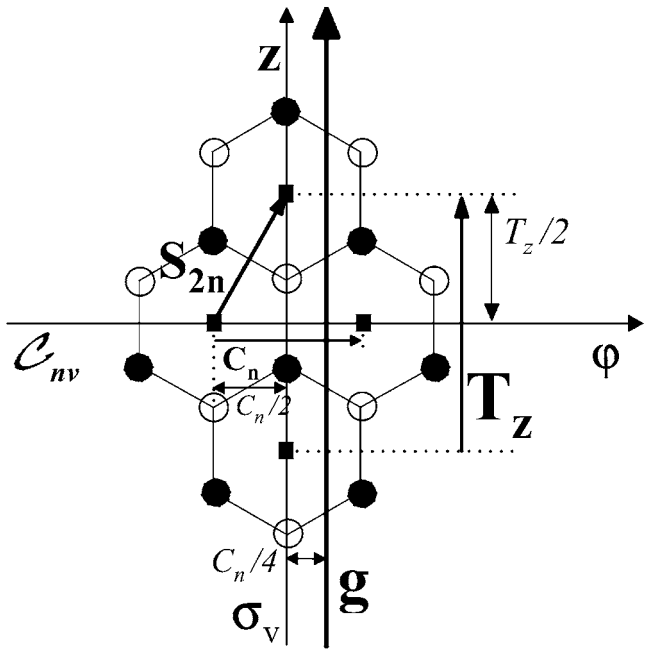

Figure 4. 2D projection of various symmetries of zigzag BNTs (●, B; ○, N): $\boldsymbol{T}_z$ is the primitive translation; $\boldsymbol{S}_{2n}$ is the screw axis with non-primitive translation and rotation, denoted by $T_z/2$ and $C_n/2$, respectively; $\boldsymbol{g}$ is a glide plane; $\mathcal{C}_{n\mathrm{v}}$ stands for the corresponding point-group operations, among which $\boldsymbol{\sigma}_\mathrm{v}$ and $\boldsymbol{C}_n$ are denoted.

the set relation $\mathcal{C}_{n\mathrm{h}}|_{z=0} \cap \mathcal{S}_{2n}|_{z=T_z/4} = \mathcal{C}_n$, which is valid for all n. Note that, while $p3m1$ does not possess the inversion symmetry, $\mathcal{G}^{\mathrm{arm}}[n]$ do possess this symmetry both for even and odd n!

In addition, let us point out that the buckling of B–N bonds [8, 10] has no effect on the spatial symmetries of BNTs because the B and N atoms form two concentric cylinders [10] in the BNTs. The point group of the rod group is readily obtained from equation (23):

$$\mathcal{G}_0^{\rm arm}[n] = \mathcal{C}_{n\rm h} \times [\boldsymbol{E} \oplus C_{2n}] = \mathcal{S}_{2n} \times [\boldsymbol{E} \oplus C_{2n}] = \mathcal{C}_{2n\rm h}. \tag{24}$$

Similarly, the non-symmorphic rod group that describes the $(n, 0)$ zigzag BNT with (either odd or even) index n [23, 24] can be decomposed in the following manner (the 8th family of rod groups [19]):

$$\mathcal{G}^{\rm zig}[n] = \mathcal{L}_{T_z} \times \mathcal{C}_{n\rm v} \times [\boldsymbol{E} \oplus \boldsymbol{S}_{2n}]. \tag{25}$$

Note that the glide planes in zigzag CNTs (see figure 2 (bottom) and equation (5)) are preserved in zigzag BNTs (see figure 4 and equation (25)). The point group of the rod group is readily obtained from equation (25):

$$\mathcal{G}_0^{\rm zig}[n] = \mathcal{C}_{n\rm v} \times [\boldsymbol{E} \oplus C_{2n}] = \mathcal{C}_{2n\rm v}. \tag{26}$$

To determine the symmetries (at the Γ-point) of the $6N$ phonon modes in armchair BNTs and how many modes are Raman or IR active, we have to associate them with the irreps of $\mathcal{G}_0^{\rm arm}[n] = \mathcal{C}_{2n\rm h}$. Recall that the character table of $\mathcal{C}_{2n\rm h}$ possesses $4n$ irreps [21]:

$$\Gamma_{\mathcal{C}_{2n\rm h}} = {\rm A_g} \oplus {\rm B_g} \oplus {\rm A_u} \oplus {\rm B_u} \oplus \mathop{\Large\oplus}_{j=1}^{n-1} \{{\rm E}_{j\rm g}^{\pm} \oplus {\rm E}_{j\rm u}^{\pm}\}. \tag{27}$$

The $6N$ phonon modes transform according to the following irreps:

$$\begin{aligned}\Gamma_{6N}^{\rm arm} = \Gamma_{\rm a}^{\rm arm} \otimes \Gamma_{\rm v} = {} & 4{\rm A_g} \oplus 2{\rm B_g} \oplus 2{\rm A_u} \oplus 4{\rm B_u} \\ & \oplus 2{\rm E}_{1\rm g}^{\pm} \oplus 4{\rm E}_{2\rm g}^{\pm} \oplus 2{\rm E}_{3\rm g}^{\pm} \oplus \cdots \oplus (3 + (-1)^{n-1}){\rm E}_{(n-1)\rm g}^{\pm} \\ & \oplus 4{\rm E}_{1\rm u}^{\pm} \oplus 2{\rm E}_{2\rm u}^{\pm} \oplus 4{\rm E}_{3\rm u}^{\pm} \oplus \cdots \oplus (3 - (-1)^{n-1}){\rm E}_{(n-1)\rm u}^{\pm},\end{aligned} \tag{28}$$

where

$$\Gamma_{\rm a}^{\rm arm} = 2\left({\rm A_g} \oplus {\rm B_u} \oplus \mathop{\Large\oplus}_{j=2l}^{n-1} {\rm E}_{j\rm g}^{\pm} \oplus \mathop{\Large\oplus}_{j=2l-1}^{n-1} {\rm E}_{j\rm u}^{\pm}\right), \tag{29}$$

stands for the reducible representations of the positions of B and N atoms inside the unit cell. The prefactor of 2 in $\Gamma_{\rm a}^{\rm arm}$ (29) reflects the two equivalent and disjoint sub-lattices formed by the B and N atoms in the BNTs. $\Gamma_{\rm v} = {\rm A_u} \oplus {\rm E}_{1\rm u}^{\pm}$ is the vector representation. Of these modes, the ones that transform according to $\Gamma_{\rm t} = {\rm A_g} \oplus {\rm E}_{1\rm g}^{\pm} \oplus {\rm E}_{2\rm g}^{\pm}$ (the tensor representation) or $\Gamma_{\rm v}$ are Raman or IR active, respectively. Out of the $6N$ phonon modes, four (which transform as $\Gamma_{\rm v}$ and $\Gamma_{R_z} = {\rm A_g}$) have vanishing frequencies [22]. Consequently, the symmetries and numbers of optically active phonon modes in armchair BNTs are given by [24]:

$$\Gamma_{\rm Raman}^{\rm arm} = 3{\rm A_g} \oplus 2{\rm E}_{1\rm g}^{\pm} \oplus 4{\rm E}_{2\rm g}^{\pm} \Longrightarrow n_{\rm Raman}^{\rm arm} = 9, \tag{30}$$

$$\Gamma_{\rm IR}^{\rm arm} = {\rm A_u} \oplus 3{\rm E}_{1\rm u}^{\pm} \Longrightarrow n_{\rm IR}^{\rm arm} = 4. \tag{31}$$

Note that the numbers of Raman- and IR-active phonon modes found for armchair BNTs are almost the same as for armchair CNTs (eight Raman and three IR active modes; see section 2).

Analogously to the treatment given above for armchair BNTs, we would like to discuss the irreps of $\mathcal{G}_0^{\rm zig}[n] = \mathcal{C}_{2n\rm v}$. Recall that the character table of $\mathcal{C}_{2n\rm v}$ possesses $n + 3$ irreps [21]:

$$\Gamma_{\mathcal{C}_{2n\rm v}} = {\rm A}_1 \oplus {\rm A}_2 \oplus {\rm B}_1 \oplus {\rm B}_2 \oplus \mathop{\Large\oplus}_{j=1}^{n-1} {\rm E}_j. \tag{32}$$

The $6N$ phonon modes transform according to the following irreps:

$$\Gamma_{6N}^{\mathrm{zig}} = \Gamma_{\mathrm{a}}^{\mathrm{zig}} \otimes \Gamma_{\mathrm{v}} = 4\mathrm{A}_1 \oplus 2\mathrm{A}_2 \oplus 4\mathrm{B}_1 \oplus 2\mathrm{B}_2 \oplus \sum_{j=1}^{n-1} 6\mathrm{E}_j, \tag{33}$$

where

$$\Gamma_{\mathrm{a}}^{\mathrm{zig}} = 2\left(\mathrm{A}_1 \oplus \mathrm{B}_1 \oplus \sum_{j=1}^{n-1} \mathrm{E}_j\right) \tag{34}$$

and $\Gamma_{\mathrm{v}} = \mathrm{A}_1 \oplus \mathrm{E}_1$. Of these modes, the ones that transform according to $\Gamma_{\mathrm{t}} = \mathrm{A}_1 \oplus \mathrm{E}_1 \oplus \mathrm{E}_2$ and/or Γ_{v} are Raman and/or IR active, respectively. Four of the $6N$ phonon modes—those which transform as Γ_{v} and $\Gamma_{R_z} = \mathrm{A}_2$—have vanishing frequencies [22]. Consequently, the symmetries and numbers of optically active phonon modes in zigzag BNTs are given by [24]:

$$\Gamma_{\mathrm{Raman}}^{\mathrm{zig}} = 3\mathrm{A}_1 \oplus 5\mathrm{E}_1 \oplus 6\mathrm{E}_2 \Longrightarrow n_{\mathrm{Raman}}^{\mathrm{zig}} = 14, \tag{35}$$

$$\Gamma_{\mathrm{IR}}^{\mathrm{zig}} = 3\mathrm{A}_1 \oplus 5\mathrm{E}_1 \Longrightarrow n_{\mathrm{IR}}^{\mathrm{zig}} = 8. \tag{36}$$

Note that the numbers of Raman- and IR-active phonon modes found for zigzag BNTs are almost twice those for zigzag CNTs (eight Raman- and three IR-active modes; see section 2) or armchair BNTs (see equations (30) and (31)). In addition, as a result of the lowered symmetry with respect to—and in contrast to—the situation for zigzag CNTs, *all* eight IR-active modes are Raman-active as well.

3.2. Chiral boron nitride nanotubes

Finally, let us discuss the (n, m) chiral BNT. Following the lack of C_2 axes in $p3m1$, the $\mathcal{D}_d$ point group in the (n, m) chiral CNT (see equation (16)) reduces to $\mathcal{C}_d$ in the (n, m) chiral BNT. Nevertheless, the (n, m) chiral BNT still possesses the non-symmorphic rod-group symmetries, because the screw axis $\boldsymbol{S}_N$ 'survives' the above symmetry lowering. Consequently, the non-symmorphic rod group that describes the (n, m) chiral BNT [23, 24] can be decomposed as follows (the first family of rod groups [19]):

$$\mathcal{G}^{\mathrm{ch}}[N] = \mathcal{L}_{T_z} \times \mathcal{C}_d \times \left[\sum_{j=0}^{\frac{N}{d}-1} \boldsymbol{S}_{N/d}^{j}\right] = \mathcal{L}_{T_z} \times \left[\sum_{j=0}^{N-1} \boldsymbol{S}_{N}^{j}\right]. \tag{37}$$

From equation (37) we can easily find the point group of the rod group:

$$\mathcal{G}_0^{\mathrm{ch}}[N] = \mathcal{C}_d \times \left[\sum_{j=0}^{\frac{N}{d}-1} C_{N/d}^{j}\right] = \sum_{j=0}^{N-1} C_N^j = \mathcal{C}_N. \tag{38}$$

To determine the symmetries (at the Γ-point) of the $6N$ phonon modes in chiral BNTs and how many modes are Raman and/or IR active, we have to associate them with the irreps of $\mathcal{G}_0^{\mathrm{ch}}[N] = \mathcal{C}_N$. Recall that the character table of $\mathcal{C}_N$ possesses N irreps [21]:

$$\Gamma_{\mathcal{C}_N} = \mathrm{A} \oplus \mathrm{B} \oplus \sum_{j=1}^{\frac{N}{2}-1} \mathrm{E}_j^{\pm}. \tag{39}$$

The $6N$ phonon modes transform according to the following irreps:

$$\Gamma_{6N}^{\mathrm{ch}} = \Gamma_{\mathrm{a}}^{\mathrm{ch}} \otimes \Gamma_{\mathrm{v}} = 6\mathrm{A} \oplus 6\mathrm{B} \oplus \sum_{j=1}^{\frac{N}{2}-1} 6\mathrm{E}_j^{\pm}, \tag{40}$$

where

$$\Gamma_{\rm a}^{\rm ch} = 2\left(\mathrm{A} \oplus \mathrm{B} \oplus \sum_{j=1}^{\frac{N}{2}-1} \mathrm{E}_j^{\pm}\right) = 2\Gamma_{\mathcal{C}_N} \tag{41}$$

and $\Gamma_{\rm v} = \mathrm{A} \oplus \mathrm{E}_1^{\pm}$. Of these modes, the ones that transform according to $\Gamma_{\rm t} = \mathrm{A} \oplus \mathrm{E}_1^{\pm} \oplus \mathrm{E}_2^{\pm}$ and/or $\Gamma_{\rm v}$ are Raman and/or IR active, respectively. Four of the $6N$ phonon modes—those which transform as $\Gamma_{\rm v}$ and $\Gamma_{R_z} = \mathrm{A}$—have vanishing frequencies [22]. Consequently, the symmetries and numbers of optically active phonon modes are given by [24]:

$$\Gamma_{\rm Raman}^{\rm ch} = 4\mathrm{A} \oplus 5\mathrm{E}_1^{\pm} \oplus 6\mathrm{E}_2^{\pm} \Longrightarrow n_{\rm Raman}^{\rm zig} = 15, \tag{42}$$

$$\Gamma_{\rm IR}^{\rm ch} = 4\mathrm{A} \oplus 5\mathrm{E}_1^{\pm} \Longrightarrow n_{\rm IR}^{\rm zig} = 9. \tag{43}$$

Note that the numbers of Raman- and IR-active phonon modes found for chiral BNTs are almost the same as for chiral CNTs (14 Raman- and six IR-active modes; see section 2).

4. Concluding remarks

The connection between spatial symmetry and the numbers of Raman- and IR-active vibrations in single-walled nanotubes, in particular for CNTs and BNTs, has been a stimulating problem over the past several years. The accounts given here show that classical molecular spectroscopy principles have certainly had contemporary success in—and relevance to—the subject. In particular, by utilizing the latterly identified higher-symmetric factor group $\mathcal{D}_{2n\rm h}$ for the symmetry analysis of phonon modes in achiral CNTs, it has been shown that the numbers of Raman- and IR-active vibrations is about half of what was previously predicted, in conjunction with experimental results (see, for example, [14, 15]). The most recent experiments on the IR and Raman spectroscopy of BNTs [26] also reflect the basic theoretical tools reviewed in this work.

Acknowledgments

The author wishes to thank: Professor L S Cederbaum for discussions; Professor N Moiseyev, Dr V Averbukh and Professor U Peskin from the Technion, Haifa (where this work was originated) for many fruitful discussions; and Professors S Bellucci and M De Crescenzi for their kind hospitality at N&N 2001, Frascati, Italy. OEA would like to thank the European Community (Marie-Curie Fellowship) for current support.

References

[1] Iijima S 1991 *Nature* **345** 56
[2] Dekker C 1999 *Phys. Today* **52** 22
[3] Terrones M, Hsu W K, Kroto H W and Walton D R M 1999 *Top. Curr. Chem.* **199** 189
[4] Saito R, Dresselhaus G and Dresselhaus M S 1998 *Physical Properties of Carbon Nanotubes* (London: Imperial College Press)
[5] Chopra N G, Luyken R J, Cherrey K, Crespi V H, Cohen M L, Louie S G and Zettl A 1995 *Science* **269** 966
[6] Yu D P, Sun X S, Lee C S, Bello I, Lee S T, Gu H D, Leung K M, Zhou G W, Dong Z F and Zhang Z 1998 *Appl. Phys. Lett.* **72** 1966
[7] Rubio A, Corkill J L and Cohen M L 1994 *Phys. Rev.* B **49** 5081
[8] Blase X, Rubio A, Louie S G and Cohen M L 1994 *Europhys. Lett.* **28** 335
[9] Chopra N G and Zettl A 1998 *Solid State Commun.* **105** 297
[10] Menon M and Srivastava D 1999 *Chem. Phys. Lett.* **307** 407
[11] Dubay O and Kresse G 2003 *Phys. Rev.* B **67** 035401

[12] Saito R, Takeya T, Kimura T, Dresselhaus G and Dresselhaus M S 1998 *Phys. Rev.* B **57** 4145
[13] Saito R, Takeya T, Kimura T, Dresselhaus G and Dresselhaus M S 1999 *Phys. Rev.* B **59** 2388
[14] Rao A M, Richter E, Bandow S, Chase B, Eklund P C, Williams K A, Fang S, Subbaswamy K R, Menon M, Thess A, Smalley R E, Dresselhaus G and Dresselhaus M S 1997 *Science* **275** 187
[15] Journet C, Maser W K, Bernier P, Loiseau A, Lamy de la Chapells M, Lefrant S, Deniard P, Lee R and Fischer J E 1997 *Nature* **388** 756
[16] Damnjanović M, Milošević I, Vuković T and Sredanović R 1999 *Phys. Rev.* B **60** 2728
[17] Damnjanović M, Milošević I, Vuković T and Sredanović R 1999 *J. Phys. A: Math. Gen.* **32** 4097
[18] Alon O E 2001 *Phys. Rev.* B **63** 201403(R)
[19] Damnjanović M and Vujičić M 1982 *Phys. Rev.* B **25** 6987
[20] Cornwell J F 1969 *Group Theory and Electronic Energy Bands in Solids* (Amsterdam: North-Holland)
[21] Harris D C and Bertolucci M D 1989 *Symmetry and Spectroscopy: an Introduction to Vibrational and Electronic Spectroscopy* (New York: Dover)
[22] Liang C Y and Krimm S 1956 *J. Chem. Phys.* **25** 543
[23] Damnjanović M, Vuković T, Milošević I and Nikolić B 2001 *Acta Crystallogr.* A **57** 304
[24] Alon O E 2001 *Phys. Rev.* B **64** 153408
[25] Král P, Mele E J and Tománek D 2000 *Phys. Rev. Lett.* **85** 1512
[26] Arenal de la Concha R, Wirtz L, Mevellec J-Y, Lefrant S, Loiseau A and Rubio A 2003 unpublished
[27] Sánchez-Portal D and Hernández E 2002 *Phys. Rev.* B **66** 235415
[28] Popov V N 2003 *Phys. Rev.* B **67** 085408
[29] Wirtz L, Arenal de la Concha R, Loiseau A and Rubio A 2003 *Phys. Rev.* B **68** 045425